

Theory of Toeplitz Determinants and the Spin Correlations of the Two-Dimensional Ising Model. V

BARRY M. MCCOY

Institute for Theoretical Physics, State University of New York, Stony Brook, New York 11790

AND

TAI TSUN WU*

Gordon McKay Laboratory, Harvard University, Cambridge, Massachusetts 02138

(Received 8 April 1968)

In a previous paper of this series, we studied $\mathfrak{P}(\bar{\sigma})$, the probability that the average boundary spin for a half-plane of Ising spins is $\bar{\sigma}$. We extend our study of such functions by generalizing the previous derivation to any magnetic system and using them to relate the magnetic behavior at the critical isotherm to the spin-spin correlations at the critical temperature. We also clarify the meaning of the secondary maxima previously found in $\mathfrak{P}(\bar{\sigma})$ by a more accurate calculation and by examining the magnetization on interior rows of the half-plane. These considerations show that $\mathfrak{P}(\bar{\sigma})$ is more properly to be considered as the sum of two separate spin probability functions. The various ways in which the thermodynamic limit may be taken and the effects that these different limiting procedures have on $\mathfrak{P}(\bar{\sigma})$ are discussed in detail. The influence of boundary conditions on spin probability functions is studied by reversing the sign of one column of horizontal bonds. We compute the additional free energy resulting from the misfit bonds and use this to show that $\mathfrak{P}(\bar{\sigma})$ is no longer bimodal but is rectangular for $|\bar{\sigma}|$ less than the boundary spontaneous magnetization. Finally, we present in graphical form numerical integrations of the boundary magnetization and susceptibility.

1. INTRODUCTION

IN a previous paper of this series,¹ we obtain some of the properties of a half-plane of Ising spins interacting with a magnetic field \mathfrak{H} applied to one boundary row only. In the course of this discussion, we compute $\mathfrak{P}(\bar{\sigma})$, the probability that at zero magnetic field the average boundary spin is $\bar{\sigma}$. Our purpose is to help interpret the fact that the boundary magnetization \mathfrak{M}_1 , while discontinuous at $\mathfrak{H}=0$, may be analytically continued beyond $\mathfrak{H}=0$ to give a hysteresis loop. It is the purpose of this paper to make more precise the discussion of $\mathfrak{P}(\bar{\sigma})$ both by a more accurate evaluation and by expanding our point of view to more general situations than the half-plane.

We begin our discussion of spin probability functions in Sec. 2 by noting that our previous derivation of $\mathfrak{P}(\bar{\sigma})$ is not restricted to the half-plane but holds for the spin probability function of any magnetic system. We obtain a first approximation to this probability function and use it to relate the behavior of the magnetization at $T=T_c$ near $H=0$ to the spin-spin correlation function at T_c . In particular, if

$$M \rightarrow \text{sgn}(H)K |H|^{1/\delta} \quad (1.1)$$

and as $r \rightarrow \infty$

$$\langle \sigma_0 \sigma_r \rangle \rightarrow c r^{2-d-\eta}, \quad (1.2)$$

where r is the separation between spins and d is the

dimension of the lattice, we find²

$$\delta = \max[1, 2d(d-2+\eta)^{-1} - 1]. \quad (1.3)$$

The meanings of δ and η in this formula are discussed in Sec. 2. If we apply (1.3) to existing numerical data, we find that $\delta=15$ for the two-dimensional Ising model, in excellent agreement with previous work.³ In three dimensions, (1.3) is not quite satisfied by present values of $\delta=5.20 \pm 0.15$ and $\eta=0.056 \pm 0.008$,⁴ and we speculate that the disagreement is due to the appearance of further singularities such as logarithms in (1.1) and (1.2).⁵

In Sec. 3, we indicate how the asymptotic-series evaluation of $P(\bar{\sigma})$ is related to a cluster expansion in terms of spin correlation functions. From these general considerations, we turn, in Sec. 4, to the specific example of the half-plane problem and derive an approximation to the boundary-spin probability function for a lattice with a finite number of rows and columns. This gives us the opportunity to examine explicitly how the various ways of taking the thermodynamic limit affect the spin probability function. This derivation makes clear that below T_c , $\mathfrak{P}(\bar{\sigma})$ consists of two terms, one exponentially smaller than the other. We examine the analytic continuation past $\mathfrak{H}=0$ of the magnetization of all interior rows to show

² This relation seems to have been first stated by M. E. Fisher, *J. Appl. Phys.* **38**, 981 (1967). While this manuscript was in preparation, other derivations have been published by J. Gunton and M. Buckingham, *Phys. Rev. Letters* **20**, 143 (1968); and G. Stell, *ibid.* **20**, 533 (1968).

³ D. S. Gaunt, M. E. Fisher, M. F. Sykes, and J. W. Essam, *Phys. Rev. Letters* **13**, 713 (1964).

⁴ M. E. Fisher and R. J. Burford, *Phys. Rev.* **156**, 583 (1967); L. Kadanoff *et al.*, *Rev. Mod. Phys.* **39**, 395 (1967).

⁵ See also G. Stell (Ref. 2).

* Supported in part by National Science Foundation Grant No. GP-5321.

¹ B. M. McCoy and T. T. Wu, *Phys. Rev.* **162**, 436 (1967). This paper will henceforth be referred to as IV.

that these two contributions to $\mathfrak{P}(\bar{\sigma})$ have separate interpretations; they differ in the direction in which the bulk spin is pointing. In IV, it was unclear how far the boundary magnetization would follow its analytic continuation when \mathfrak{S} was decreased from ∞ to negative values. We are now able to conclude that the boundary magnetization will follow its analytic continuation until the bulk magnetization flips over. The value of \mathfrak{S} at which this occurs is the same \mathfrak{S} at which the analytic continuation of the magnetization of each row equals the stable value of the magnetization.

In Sec. 5, we show how a slight modification of boundary conditions can radically alter the behavior of $\mathfrak{P}(\bar{\sigma})$ when $|\bar{\sigma}| < \mathfrak{M}_1(0)$. We modify the lattice of IV by replacing one column of horizontal bonds E_1 with bonds $-E_1$ and find that when the number of rows is infinite, the boundary spin probability function at $\mathfrak{S}=0$, instead of being bimodal, is essentially constant for $|\bar{\sigma}| < \mathfrak{M}_1(0)$. This expected flat distribution is due to the presence of two domains of opposite spin, one of whose boundaries is fixed at the position of the mis-

matched bond, while the other may be between any two columns of the lattice.

We conclude this discussion of boundary effects in Sec. 6, with some graphical presentation of numerical integrations of the boundary magnetization and susceptibility. These curves are quite useful in supplementing the nonanalytic part of the behavior near T_c by explicitly evaluating the integrals in a region where no compact approximation is available. In particular, we find that for $\mathfrak{S} \neq 0$ at $T=T_c$ the boundary magnetization and susceptibility are quite smooth in appearance even though the second derivative is infinite.

2. CRITICAL ISOTHERM

Consider any magnetic system interacting with an external field H . We wish to study the probability $P(\bar{\sigma})$ that, when $H=0$, the average of the spins which can interact with the magnetic field is $\bar{\sigma}$. Denote the relevant spin variable of the j th site by σ_j . Then, if \mathfrak{N} spins interact with H and $|\frac{1}{2}\mathfrak{N}\bar{\sigma}|$ is an integer not larger than $\frac{1}{2}\mathfrak{N}$,

$$\begin{aligned}
 P(\bar{\sigma}) &= \langle \delta(\sum_{j=1}^{\mathfrak{N}} \sigma_j - \mathfrak{N}\bar{\sigma}) \rangle \\
 &= (2\mathfrak{N}+a)^{-1} \sum_{k'=1}^{2\mathfrak{N}+a} \langle \exp[2\pi i k' (2\mathfrak{N}+a)^{-1} (\sum_{k=1}^{\mathfrak{N}} \sigma_j - \mathfrak{N}\bar{\sigma})] \rangle \\
 &= (2\mathfrak{N}+a)^{-1} Z(0)^{-1} \sum_{k=1}^{2\mathfrak{N}+a} \exp[-2\pi i k (2\mathfrak{N}+a)^{-1} \mathfrak{N}\bar{\sigma}] Z[2\pi i k (2\mathfrak{N}+a)^{-1} \beta^{-1}], \tag{2.1}
 \end{aligned}$$

where $Z(H)$ is the partition function of the system, a is an arbitrary positive integer, and δ is the Kronecker δ . If we write

$$Z(H) = \exp[-\beta \mathfrak{N} F(H)] Z(0), \tag{2.2}$$

where $F(H)$ is the part of the free energy that depends on magnetic field, and convert the sum in (2.1) to an integral, we have

$$P(\bar{\sigma}) = -i\beta(2\pi)^{-1} \int_{-i\pi/\beta}^{i\pi/\beta} d\xi \exp\{-\mathfrak{N}\beta[\xi\bar{\sigma} + F(\xi)]\}. \tag{2.3}$$

We may obtain an asymptotic approximation to (2.3) as $\mathfrak{N} \rightarrow \infty$ by the method of steepest descents. The point of steepest descent is determined from

$$\bar{\sigma} = -F'(\xi_0) = M(\xi_0). \tag{2.4}$$

On the assumption that $F(H)$ has a sufficiently large region of analyticity so that we can deform the contour to the steepest-descent path, we find

$$P(\bar{\sigma}) \sim \frac{1}{4} [2\beta\chi(\xi_0)/\mathfrak{N}\pi]^{1/2} \exp(\mathfrak{N}W), \tag{2.5}$$

where

$$W = -\beta[\xi_0\bar{\sigma} + F(\xi_0)] \tag{2.6a}$$

and

$$\chi(\xi_0) = M'(\xi_0). \tag{2.6b}$$

We may now derive (1.3) by calculating the second moment of $P(\bar{\sigma})$ at $T=T_c$ and $H=0$. If we make the assumption (1.1) that $M \sim K \operatorname{sgn}(H) |H|^{1/\delta}$ at $T=T_c$ as $H \rightarrow 0$, then

$$F(H) \sim -K\delta(\delta+1)^{-1} |H|^{1+1/\delta}, \tag{2.7}$$

$$\xi_0 \sim \operatorname{sgn}(\bar{\sigma}) (K^{-1} |\bar{\sigma}|)^\delta, \tag{2.8}$$

and, as $\mathfrak{N} \rightarrow \infty$,

$$P(\bar{\sigma}) \sim \text{const} \times \exp[-\beta\mathfrak{N}K^{-\delta}(\delta+1)^{-1} |\bar{\sigma}|^{\delta+1}]. \tag{2.9}$$

We therefore obtain, as $\mathfrak{N} \rightarrow \infty$,

$$\begin{aligned}
 \int_{-1}^1 P(\bar{\sigma}) \bar{\sigma}^2 d\bar{\sigma} &\sim [(\delta+1)K^\delta/(\beta\mathfrak{N})]^{2/(\delta+1)} \int_{-\infty}^{\infty} x^2 \\
 &\times \exp(-|x|^{\delta+1}) dx \left[\int_{-\infty}^{\infty} \exp(-|x|^{\delta+1}) dx \right]^{-1}. \tag{2.10}
 \end{aligned}$$

We may also write, as $\mathfrak{N} \rightarrow \infty$,

$$\int_{-1}^1 P(\bar{\sigma}) \bar{\sigma}^2 d\bar{\sigma} \sim \mathfrak{N}^{-2} \sum_{j=1}^{\mathfrak{N}} \sum_{k=1}^{\mathfrak{N}} \langle \sigma_j \sigma_k \rangle. \quad (2.11)$$

Using the form (1.2) for $\langle \sigma_j \sigma_k \rangle$ when the separation between the spins is large (we may neglect terms arising from short-range order, since they contribute to a lower order in \mathfrak{N} than the terms that we are retaining), we have (on the assumption that $\eta \leq 2$), as $\mathfrak{N} \rightarrow \infty$,

$$\int_{-1}^1 P(\bar{\sigma}) \bar{\sigma}^2 d\bar{\sigma} \sim c \mathfrak{N}^{-2} \sum r^{2-d-\eta} = c' \mathfrak{N}^{-1+(2-\eta)/d}. \quad (2.12)$$

We equate (2.10) and (2.12) and see that, for the \mathfrak{N} dependence of each side to be the same, we must have

$$-2(\delta+1)^{-1} = (2-\eta)d^{-1} - 1, \quad (2.13)$$

which implies

$$\delta = 2d(\eta+d-2)^{-1} - 1. \quad (2.14)$$

If $\eta > 2$, the sum in (2.12) converges and δ must be equal to 1.

We must now understand precisely what the forms (1.1) and (1.2) mean for a finite lattice. Conventionally, T_c and critical exponents like δ and η are defined only in an infinite lattice. Indeed, for a finite lattice, we know that all thermodynamic functions must be analytic, because the partition function is the sum of a finite number of terms. However, it is clear physically that (1.2) will have meaning for a finite lattice if we set $T = T_c$ of the bulk. If r is much larger than the separation between sites but much smaller than the smallest lattice dimension, then (1.2) must hold with the same η as the exponent in the limit $\mathfrak{N} \rightarrow \infty$. If r and \mathfrak{N} go to ∞ proportionally, however, while we expect some form similar to (1.2) to hold, it is not necessarily the case that the η so defined will be the same as the η previously obtained. Even if the two η 's are the same, there is every reason to suppose that the proportionality constant in (1.2) will now acquire an angular dependence which is determined by the shape of the lattice. A similar discussion applies to the exponent δ .

In spite of these ambiguities, let us make the very plausible assumption that the δ and η which appear in (2.14) are equal to the corresponding values for the infinite lattice. Using the known value of $\eta = \frac{1}{4}$ for the two-dimensional Ising model, we obtain $\delta = 15$, in excellent agreement with the previous numerical value³ of 15.00 ± 0.02 . Moreover, we know from (2.9) that for the two-dimensional Ising model at $T = T_c$

$$P(\bar{\sigma}) \sim \text{const} \times \exp(-\text{const} \times \mathfrak{N} |\bar{\sigma}|^{16}). \quad (2.15)$$

However, for the three-dimensional Ising model, the numerical estimates⁴ of $\delta = 5.2 \pm 0.15$ and $\eta = 0.056 \pm 0.008$ do not satisfy (2.14). In order to resolve this discrepancy, we speculate that it is the forms (1.1) and

(1.2) that are incorrect. The simplest modification to make is

$$M \sim \text{sgn}(H) K |H|^{1/\delta} |\ln |H||^{\Lambda'/\delta} \quad (2.16)$$

and

$$\langle \sigma_0 \sigma_r \rangle \sim c r^{2-d-\eta} (\ln r)^{-\Lambda}. \quad (2.17)$$

Then, as $\mathfrak{N} \rightarrow \infty$, (2.10) is replaced with

$$\int_{-1}^1 P(\bar{\sigma}) \bar{\sigma}^2 d\bar{\sigma} \sim K' [\mathfrak{N} (\ln \mathfrak{N})^{\Lambda'}]^{-2/(\delta+1)} \quad (2.10')$$

and (2.12) is replaced with

$$\int_{-1}^1 P(\bar{\sigma}) \bar{\sigma}^2 d\bar{\sigma} \sim c' [\mathfrak{N}^{1/d} (\ln \mathfrak{N})^{\Lambda}]^{-2+d+\eta}, \quad (2.12')$$

from which, besides (2.14), we deduce

$$\Lambda' = d\Lambda. \quad (2.18)$$

In doing a numerical calculation of δ and η , unless extreme care is used, a logarithm cannot be distinguished from a small power law. Therefore, if we replaced $\ln |H|$ with $-|H|^{-\epsilon}$ as $|H| \rightarrow 0$ and $\ln r$ with $r^{\epsilon'}$ as $r \rightarrow \infty$, where ϵ and ϵ' are positive, we would find an "effective" δ and η of

$$\delta_{\text{eff}} = \delta(1 - 3\Lambda\epsilon)^{-1} \quad (2.19)$$

and

$$2 - d - \eta_{\text{eff}} = (2 - d - \eta)(1 + \Lambda\epsilon'). \quad (2.20)$$

Here δ_{eff} and η_{eff} are to be the existing numerical values. If we assume that $\epsilon = \epsilon'$, then we find that $\Lambda\epsilon = 0.026$, $\delta = 4.78$, and $\eta = 0.03$ are consistent with the existing values of δ_{eff} and η_{eff} . There is, however, no reason to assume that $\epsilon = \epsilon'$ and we make the natural conjecture that $\delta = 5$ and $\eta = 0$, and that the discrepancy between these values and the existing numerical values comes from the additional singularities that (1.1) and (1.2) may possess, of which logarithms are merely one simple example.

We may slightly generalize (2.14) by assuming that the magnetic field does not interact with the entire d -dimensional lattice but only with a d_1 -dimensional sublattice. We find in this case

$$\delta = \max[2d_1(\eta+d-2)^{-1} - 1, 1]. \quad (2.21)$$

If we assume that this δ and η are the infinite-lattice values, we find that for a magnetic field interacting with a row of spins in the interior of a two-dimensional Ising lattice, the magnetization of the sites interacting with the field behaves as $\text{sgn}(H) |H|^{1/7}$ at $T = T_c$ and H near zero. This is to be contrasted with the $-\mathfrak{N} \ln |\mathfrak{N}|$ behavior of the boundary magnetization found in IV.

We give an alternative derivation of (2.21) which is valid for an infinite lattice by considering the behavior of the correlation functions for small H at $T = T_c$. If at $T = T_c$ the correlation functions are integrable, M goes analytically to zero as H goes to zero and $\delta = 1$. We therefore exclude this case and assume that the

correlation functions are not integrable at $T=T_c$ and $H=0$. However, even at $T=T_c$ when $H \neq 0$, the correlation functions approach the limiting value of M^2 in an integrable fashion for sufficiently large separations. For values of the separation that are not so large, however, $\langle \sigma_0 \sigma_r \rangle$ is approximated by the nonintegrable $T=T_c, H=0$ value. The distance r_0 which separates these two regions depends on H and may be defined in two separate ways. We can define the correlation-length exponent κ to be $H^{-\kappa} = r_0$ such that the correlation function may be expanded as a function of $rH^\kappa = \text{const}$ as $r \rightarrow \infty$ and $H \rightarrow 0$. [For the case of the boundary correlation function $\kappa=2$, see Eq. (8.90) of IV.] By studying the divergence as $H \rightarrow 0$ of

$$\chi = KH^{-1+1/\delta} = \sum_{r=0}^{\infty} (\langle \sigma_0 \sigma_r \rangle - M^2) \sim \sum_{r=0}^{r_0} cr^{-(d-2+\eta)}, \quad (2.22)$$

where the sums are over the d_1 -dimensional subspace whose spins interact with H , we find

$$\kappa = (\delta - 1)(d_1 - d - \eta + 2)^{-1} \delta^{-1}. \quad (2.23)$$

Alternatively, we may also define $r_0' = H^{-\kappa'}$ as the value of the separation when the $T=T_c, H=0$ correlation function equals the limiting value as $r \rightarrow \infty$ of the $T=T_c, H \neq 0$ correlation function. This gives

$$cH^{-\kappa'(d-2+\eta)} = K^2 H^{2/\delta}, \quad (2.24)$$

so that

$$\kappa' = 2\delta^{-1}(d-2+\eta)^{-1}. \quad (2.25)$$

If we identify κ and κ' , we recover (2.21). This derivation is somewhat superior to the previous one because it deals only with critical exponents of the infinite lattice. However, the assumption that $\kappa = \kappa'$ is not a rigorous statement, and furthermore, the argument cannot be extended to include logarithmic terms.

For the two-dimensional Ising model, if $d_1=2$, (2.23) gives $\kappa=8/15$, while if $d_1=1, \kappa=8/7$. In the three-dimensional case, if $\delta=5$ and $\eta=0$, then $\kappa=8/5$.

We now return to the question of the finite-volume terms in $F(H)$ and in the correlation functions by exhibiting these terms for the boundary problem.

Here and in the rest of this paper, we follow the notations of IV.⁶ Consider first the evaluation of $\mathfrak{M}_1(\mathfrak{S})$ in a half-plane lattice of $2\mathfrak{N}$ columns at $T=T_c$. In (5.1) of IV, we wrote down $\mathfrak{M}_1(\mathfrak{S})$ when $\mathfrak{N} \rightarrow \infty$ by retaining only the first terms in the Poisson-sum formula

$$(2\mathfrak{N})^{-1} \sum_{n=1}^{2\mathfrak{N}} \delta[\theta - \pi(2n-1)(2\mathfrak{N})^{-1}] \\ = (2\pi)^{-1} \sum_{m=-\infty}^{\infty} (-1)^m \exp(2i\mathfrak{N}m\theta). \quad (2.26)$$

To study the finite- \mathfrak{N} case, we retain all terms in (2.26) and write

$$\mathfrak{M}_1(\mathfrak{S}) = z + (2\pi)^{-1}(1-z^2)zz_1 \\ \times \int_{-\pi}^{\pi} d\theta \sum_{m=-\infty}^{\infty} (-1)^m \exp(2i\mathfrak{N}m\theta) |1 + e^{i\theta}|^2 \\ \times [z^2 z_1 |1 + e^{i\theta}|^2 - z_2^2 |1 + z_1 e^{i\theta}|^2 + z_2(1-z_1^2)\alpha]^{-1}. \quad (2.27)$$

We wish to consider $T=T_c, z$ small, and $z^2\mathfrak{N}$ large. Then it is straightforward to see that to lowest order in $(z^2\mathfrak{N})^{-1}$

$$\mathfrak{M}_1(\mathfrak{S}) \sim -\pi^{-1}z |z_2|^{-1} [4 \ln |z| + z_2^2(2z^2\mathfrak{N})^{-2} \frac{1}{2}\pi^2], \quad (2.28)$$

so that to lowest order in $(\mathfrak{S}^2\mathfrak{N})^{-1}$

$$\mathfrak{F}(\mathfrak{S}) \sim \pi^{-1}\beta\mathfrak{S}^2 |z_2|^{-1} \\ \times [2 \ln |\beta\mathfrak{S}| + \frac{1}{2}z_2^2(2\beta^2\mathfrak{S}^2\mathfrak{N})^{-2} \frac{1}{2}\pi^2]. \quad (2.29)$$

This leads to

$$\mathfrak{F}(\bar{\sigma}) = \text{const} \times \exp\mathfrak{N}(\pi |z_2|)^{-1} \\ \times [z_2^2\pi^2\bar{\sigma}^2(8 \ln |\bar{\sigma}|)^{-1} \times \frac{1}{2}(\ln |\bar{\sigma}|)^2\bar{\sigma}^{-2}\mathfrak{N}^{-2}], \quad (2.30)$$

from which it is seen that the additional term does not contribute to the leading-order \mathfrak{N} dependence of $\langle \bar{\sigma}^2 \rangle$.

Finally, we improve the calculation of the boundary spin-spin correlation function $\mathfrak{S}_{1,1}(N, \mathfrak{S})$ at $\mathfrak{S}=0$ and $T=T_c$ when \mathfrak{N} is finite and N may be of the order of \mathfrak{N} . Retain all terms in the Poisson-sum formula to obtain the more accurate version of (8.19) of IV,

$$\mathfrak{S}_{1,1}(N, 0) = -z_2^{-1}(z_1^{-1}-z_1)(2\pi i)^{-1} \int_{\Gamma} d\xi (\xi^2-1)^{-1} \alpha^{-1} [\xi^{|N|} + \sum_{m=1}^{\infty} (-1)^m (\xi^{2\mathfrak{N}m+|N|} - \xi^{2\mathfrak{N}m-|N|})] \\ \sim \pi^{-1} |z_2|^{-1} \{ |N|^{-1} + \sum_{m=1}^{\infty} (-1)^m 2 |N| \{ |N|^2 - (2\mathfrak{N}m)^2 \}^{-1} \} \\ = |z_2|^{-1} (2\mathfrak{N})^{-1} \text{csc}[|N| \pi (2\mathfrak{N})^{-1}]. \quad (2.31)$$

If we sum this over all N , we find

$$\sum_{N=-\mathfrak{N}+1}^{\mathfrak{N}} \mathfrak{S}_{1,1}(N, 0) = 2\pi^{-1} |z_2|^{-1} \ln \mathfrak{N} + O(1) + (|z_2| \pi)^{-1} \int_0^{\pi/2} d\theta (\text{csc}\theta - \theta^{-1}) \\ = 2\pi^{-1} |z_2|^{-1} \ln \mathfrak{N} + O(1), \quad (2.32)$$

⁶ In particular, we note the definitions $z = \tanh\beta\mathfrak{S}$, $z_i = \tanh\beta E_i$ ($i=1, 2$), $\alpha_1 = z_1(1 - |z_2|)/(1 + |z_2|)$, and $\alpha_2 = z_1^{-1}(1 - |z_2|)/(1 + |z_2|)$.

so that the leading-order \mathfrak{N} dependence coming from the exact correlation function is the same as would be obtained had we omitted the terms in (2.31) that vanish when N is fixed and $\mathfrak{N} \rightarrow \infty$.

3. MOMENTS OF SPIN PROBABILITY FUNCTIONS

In Sec. 2, we dealt with questions that could be studied by use of the leading term in the asymptotic series expansion of $P(\bar{\sigma})$. Before turning to questions of secondary maxima and the manner in which the thermodynamic limit is attained for the half-plane problem, we indicate here for a general lattice how (2.3) is related to the collection of spin correlation functions of the lattice. Consider the n th moment of $P(\bar{\sigma})$. By definition,

$$\langle \bar{\sigma}^n \rangle = \mathfrak{N}^{-n} \sum \langle \sigma_i \sigma_j \cdots \sigma_l \rangle, \quad (3.1)$$

where there are n σ 's in the product and the sum is over all lattice sites. If n is odd, this moment vanishes by symmetry. If n is 2, we note that, in the two-dimensional Ising model with periodic boundary conditions,

$$\lim_{j^2+k^2 \rightarrow \infty} \langle \sigma_{00} \sigma_{jk} \rangle = M^2, \quad (3.2)$$

where M is the spontaneous magnetization.

The existence of this limit depends on the boundary conditions (see Sec. 5) but may be expected to be a general property of most lattices. In that case, we have for n even

$$\lim_{\mathfrak{N} \rightarrow \infty} \langle \bar{\sigma}^n \rangle = M^n, \quad (3.3)$$

which means that, as expected, $P(\bar{\sigma})$ consists of two

$$\begin{aligned} \langle \bar{\rho}^{2n+1} \rangle_{1/2} &= \mathfrak{N}^{-2n-1} \sum \langle \rho_i \rho_j \cdots \rho_l \rangle_{1/2} \\ &= (2n+1) 2n(2n-1) (3!)^{-1} (2n-3) (2n-5) \cdots 3 (\mathfrak{N}^{-3} \sum f_{ijk}) (\mathfrak{N}^{-2} \sum f_{ij})^{n-1} + O(\mathfrak{N}^{-n-2}). \end{aligned} \quad (3.9)$$

The leading terms in (3.8) are the even moments of a Gaussian of width $(\mathfrak{N}^{-1} \sum_j f_{0j})^{1/2}$ centered at $\bar{\rho}=0$. To this order, the odd moments (3.9) are zero. Therefore, if $T \neq T_c$ (so that $\sum_j f_{0j}$ converges) and $\bar{\sigma}$ is close enough to $\pm M$, $P(\bar{\sigma})$ is well approximated by a Gaussian. However, the important question of how close to M one must go before Gaussian behavior is obtained cannot be answered from this analysis. Finally, we may make connection with the general formula (2.3) by remarking that if we make a complete asymptotic evaluation of the integral in (2.3) and compute the moments of the resulting $P(\bar{\sigma})$ about $+M$, we shall obtain exactly the expansions (3.8) and (3.9).

4. BOUNDARY-SPIN PROBABILITY AND METASTABLE STATES

In Sec. 6 of IV, we calculated $\mathfrak{P}(\bar{\sigma})$ in the case where the number of rows ($2\mathfrak{N}$) of the half-plane was

⁷That the moments (3.3) uniquely specify $P(\bar{\sigma})$ is guaranteed by a well-known theorem. See J. A. Shohat and J. D. Tamarkin, *The Problem of Moments* (American Mathematical Society, New York, 1943), p. 11.

sharp spikes, one at each of the two values of the spontaneous magnetization.⁷

To obtain further information about the structure of these spikes, we define a new operator

$$\rho_j = \sigma_j - M \quad (3.4)$$

and consider a restricted thermal average denoted by $\langle \rangle_{1/2}$, where we average over only those states which lead to $\langle \rho_j \rangle_{1/2} = 0$. Loosely speaking, we are averaging over the half of the states that have a spontaneous magnetization of $+M$. For this special class of states, we may systematically define the functions $f_{ijk} \cdots$ as follows:

$$\langle \rho_i \rho_j \rangle_{1/2} = \langle \rho_i \rangle_{1/2} \langle \rho_j \rangle_{1/2} + f_{ij} = f_{ij}, \quad (3.5)$$

$$\langle \rho_i \rho_j \rho_k \rangle_{1/2} = f_{ijk}, \quad (3.6)$$

and

$$\langle \rho_i \rho_j \rho_k \rho_l \rangle_{1/2} = f_{ij} f_{kl} + f_{ik} f_{jl} + f_{il} f_{jk} + f_{ijkl}. \quad (3.7)$$

The $f_{ij} \cdots$ are totally symmetric functions of their indices and are constructed so that, when any two indices refer to points widely separated in space, $f_{ij} \cdots$ goes to zero. In terms of these functions, we may expand the moments of $P(\rho)$ as a series in \mathfrak{N}^{-1} . It is a simple counting problem to verify that

$$\begin{aligned} \langle \bar{\rho}^{2n} \rangle_{1/2} &= \mathfrak{N}^{-2n} \sum \langle \rho_i \rho_j \cdots \rho_l \rangle_{1/2} \\ &= (2n-1)(2n-3) \cdots 3 \mathfrak{N}^{-2n} (\sum f_{ij})^n + O(\mathfrak{N}^{-n-1}) \\ &= (2n-1)(2n-3) \cdots 3 \mathfrak{N}^{-n} (\sum f_{0j})^n + O(\mathfrak{N}^{-n-1}), \end{aligned} \quad (3.8)$$

where the last equation is only valid in a translationally invariant lattice and the $O(\mathfrak{N}^{-n-1})$ term is absent if $n=1$. Similarly,

taken to infinity before the number of columns ($2\mathfrak{N}$) was. In this case, we evaluated the leading approximation to $\mathfrak{P}(\bar{\sigma})$ and noted that we could use this $\mathfrak{S}=0$ probability function to calculate the boundary-spin probability for all \mathfrak{S} . (We remind the reader that \mathfrak{S} interacts only with the boundary row of spins.) For $|\mathfrak{S}|$ not too large, the probability function was seen to be bimodal and we interpreted the secondary maximum of the probability function as a metastable state. However, this secondary maximum disappeared when $\mathfrak{M}_1^c(\mathfrak{S})=0$, and for $|\mathfrak{S}|$ larger than this value, it was unclear from these considerations if the magnetization would follow $\mathfrak{M}_1(\mathfrak{S})$ or $\mathfrak{M}_1^c(\mathfrak{S})$. In order to resolve this question of how far the boundary magnetization will follow its analytic continuation and to study the effect of the order $\mathfrak{N} \rightarrow \infty$ followed by $\mathfrak{N} \rightarrow \infty$, we shall compute $\mathfrak{P}(\bar{\sigma}; \mathfrak{N}, \mathfrak{N})$, the boundary spin probability function at $\mathfrak{S}=0$ for finite \mathfrak{N} and \mathfrak{N} . $\mathfrak{P}(\bar{\sigma}; \mathfrak{N}, \mathfrak{N})$ is still expressed in terms of the partition function by

(2.1). From (3.26) of IV we have

$$Z_{2\mathfrak{N},\mathfrak{N}}(\mathfrak{S})/Z_{2\mathfrak{N},\mathfrak{N}}(0) = (\cosh\beta\mathfrak{S})^{4\mathfrak{N}} \prod_{\theta} \{ [1 + \alpha^{-4\mathfrak{N}}(\mathfrak{v}'/\mathfrak{v})^2]^{-1} \times [(1 - iz^2z_2^{-1}c^{-1}\mathfrak{v}'/\mathfrak{v}) + \alpha^{-4\mathfrak{N}}\mathfrak{v}'^2\mathfrak{v}^{-2}(1 + iz^2z_2^{-1}c^{-1}\mathfrak{v}'/\mathfrak{v})] \}, \quad (4.1)$$

where the product is over the $2\mathfrak{N}$ roots of -1 . Using the Poisson-sum formula (2.26), we have

$$Z_{2\mathfrak{N},\mathfrak{N}}(\mathfrak{S})/Z_{2\mathfrak{N},\mathfrak{N}}(0) = (\cosh\beta\mathfrak{S})^2 \exp\left\{ \mathfrak{N}(2\pi)^{-1} \int_{-\pi}^{\pi} d\theta \sum_{m=-\infty}^{\infty} (-1)^m \exp(2\mathfrak{N}mi\theta) \ln[(1 + \alpha^{-4\mathfrak{N}}(\mathfrak{v}'/\mathfrak{v})^2)^{-1} \times ((1 - iz^2z_2^{-1}c^{-1}\mathfrak{v}'/\mathfrak{v}) + \alpha^{-4\mathfrak{N}}(\mathfrak{v}'/\mathfrak{v})^2(1 + iz^2z_2^{-1}c^{-1}\mathfrak{v}'/\mathfrak{v}))] \right\}. \quad (4.2)$$

Define

$$\mathfrak{F}(\mathfrak{S}; \mathfrak{N}) = -\beta^{-1} \left\{ \cosh\beta\mathfrak{S} + (4\pi)^{-1} \int_{-\pi}^{\pi} d\theta \ln[(1 + \alpha^{-4\mathfrak{N}}(\mathfrak{v}'/\mathfrak{v})^2)((1 - iz^2z_2^{-1}c^{-1}\mathfrak{v}'/\mathfrak{v}) + \alpha^{-4\mathfrak{N}}(\mathfrak{v}'/\mathfrak{v})^2(1 + iz^2z_2^{-1}c^{-1}\mathfrak{v}'/\mathfrak{v}))] \right\}, \quad (4.3)$$

and define $r_{\mathfrak{N}}(\mathfrak{S})$ to be that $e^{i\theta}$ that obeys

$$(1 - iz^2z_2^{-1}c^{-1}\mathfrak{v}'/\mathfrak{v}) + \alpha^{-4\mathfrak{N}}(\mathfrak{v}'/\mathfrak{v})^2(1 + iz^2z_2^{-1}c^{-1}\mathfrak{v}'/\mathfrak{v}) = 0, \quad (4.4)$$

which approaches the r of IV when $\mathfrak{N} \rightarrow \infty$. We then see from Appendix A that for $T < T_c$

$$Z_{2\mathfrak{N},\mathfrak{N}}(\mathfrak{S})/Z_{2\mathfrak{N},\mathfrak{N}}(0) = (1 + r_{\mathfrak{N}}^{2\mathfrak{N}})[1 + r_{\mathfrak{N}}(0)^{2\mathfrak{N}}]^{-1} \exp\{-2\mathfrak{N}\beta\mathfrak{F}(\mathfrak{S}; \mathfrak{N})[1 + o(\alpha_2^{2\mathfrak{N}})]\}. \quad (4.5)$$

From Appendix A we see that $\mathfrak{F}(\mathfrak{S}; \mathfrak{N})$ has branch points at $\mathfrak{S} = i\pi n \pm \mathfrak{S}_0$, where n is an integer, \mathfrak{S}_0 is defined by $-i\mathfrak{S}_0 > 0$, $z_0 = \tanh\beta\mathfrak{S}_0$, and

$$z_0^2 = -\alpha(0)^{-4\mathfrak{N}}[1 - \alpha(0)^{-4\mathfrak{N}}]^{-1}z_2^2\mathfrak{N}_1^2. \quad (4.6)$$

If we define the cut \mathfrak{S} plane (Fig. 1) (a) by joining these branch points pairwise with cuts along the imaginary \mathfrak{S} axis such that no branch cut crosses the real axis and (b) by joining the branch points that occur for \mathfrak{S} real (\mathfrak{S} away from zero) along the real axis, then in this cut plane $\mathfrak{F}(\mathfrak{S}; \mathfrak{N})$ is analytic and obeys

$$\mathfrak{F}(\mathfrak{S}; \mathfrak{N}) = \mathfrak{F}(-\mathfrak{S}; \mathfrak{N}). \quad (4.7)$$

$\mathfrak{F}(\mathfrak{S}; \mathfrak{N})$ may be continued through this cut to $\mathfrak{F}^c(\mathfrak{S}; \mathfrak{N})$, and we find

$$\mathfrak{F}^c(\mathfrak{S}; \mathfrak{N}) - \mathfrak{F}(\mathfrak{S}; \mathfrak{N}) = -\beta^{-1} \ln r_{\mathfrak{N}}. \quad (4.8)$$

Furthermore, $r_{\mathfrak{N}}(\mathfrak{S})$ has the same branch cuts on the imaginary \mathfrak{S} axis as $\mathfrak{F}(\mathfrak{S}; \mathfrak{N})$ does, may be continued through these cuts, and obeys

$$r_{\mathfrak{N}}(\mathfrak{S}) = r_{\mathfrak{N}}(-\mathfrak{S}) = r_{\mathfrak{N}}^{-1}(\mathfrak{S}). \quad (4.9)$$

With the aid of (4.8) and (4.9) we see that, as expected, $Z_{2\mathfrak{N},\mathfrak{N}}(\mathfrak{S})$ does not have any branch points on the imaginary axis. We consider only the case $T < T_c$, where we may use (4.5) in (2.1) to obtain

$$\mathfrak{B}(\bar{\sigma}; \mathfrak{N}, \mathfrak{N}) \sim \beta(2\pi i)^{-1} \int_{-i\pi/\beta}^{i\pi/\beta} d\xi (1 + r_{\mathfrak{N}}^{2\mathfrak{N}})[1 + r_{\mathfrak{N}}(0)^{2\mathfrak{N}}]^{-1} \exp\{-2\mathfrak{N}\beta[\mathfrak{F}(\xi, \mathfrak{N}) + \xi\bar{\sigma}]\}. \quad (4.10)$$

In writing this, we have omitted the terms of $o(\alpha_2^{2\mathfrak{N}})$. Therefore terms arising from (4.10) that are smaller than $o(\alpha_2^{2\mathfrak{N}})$ must be discarded as meaningless. It is these $o(\alpha_2^{2\mathfrak{N}})$ terms that at $T = T_c$ were discussed in Sec. 2. The integral is now to be evaluated by steepest descents, where, in contrast to the less accurate expression of Sec. 6 of IV, (4.10) has *two* points of steepest descent instead of one. The integrand is analytic on the imaginary axis, so that we may deform the path to pass slightly to the right of the axis. Using (4.8), we may rewrite (4.10) as the sum of two integrals:

$$\mathfrak{B}(\bar{\sigma}; \mathfrak{N}, \mathfrak{N}) = \beta(2\pi i)^{-1} \int_{i\pi/\beta}^{i\pi/\beta} d\xi [1 + r_{\mathfrak{N}}(0)^{2\mathfrak{N}}]^{-1} \{ \exp[-2\mathfrak{N}\beta(\mathfrak{F}(\xi, \mathfrak{N}) + \xi\bar{\sigma})] + \exp[-2\mathfrak{N}\beta(\mathfrak{F}^c(\xi, \mathfrak{N}) + \xi\bar{\sigma})] \}. \quad (4.11)$$

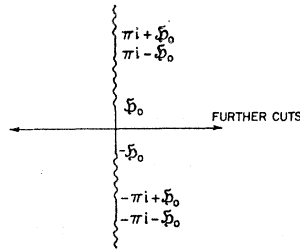


FIG. 1. Cut \mathfrak{S} plane.

When $|\bar{\sigma}| > \mathfrak{M}_1(0)$, the steepest-descent points are determined from

$$\bar{\sigma} = \mathfrak{M}_1(\xi_1; \mathfrak{N}) = -\mathfrak{F}'(\xi_1; \mathfrak{N}) \quad (4.12a)$$

and

$$\bar{\sigma} = \mathfrak{M}_1^c(\xi_2; \mathfrak{N}) = -\mathfrak{F}^c(\xi_2; \mathfrak{N}). \quad (4.12b)$$

When \mathfrak{S} is away from zero and \mathfrak{N} is large but finite, $\mathfrak{M}_1(\mathfrak{S}; \mathfrak{N})$ and $\mathfrak{M}_1^c(\mathfrak{S}; \mathfrak{N})$, as shown schematically in Fig. 2, are virtually identical with their $\mathfrak{N} \rightarrow \infty$ limits. $\mathfrak{M}_1(\mathfrak{S}; \mathfrak{N})$ has been analyzed in detail in Appendix B of IV. Define the functions

$$\mathfrak{B}_1 = -\beta[\xi\bar{\sigma} + \mathfrak{F}(\xi; \mathfrak{N})] \quad (4.13a)$$

and

$$\mathfrak{B}_2 = -\beta[\xi\bar{\sigma} + \mathfrak{F}^c(\xi; \mathfrak{N})]. \quad (4.13b)$$

Then for $|\sigma| > \mathfrak{M}_1(0)$

$$\mathfrak{P}(\bar{\sigma}; \mathfrak{N}, \mathfrak{N}) \sim [1 + r_{\mathfrak{N}}(0)^{2\mathfrak{N}}]^{-1/2} (\beta/\pi\mathfrak{N})^{1/2} \times [\chi(\xi_1)^{-1/2} \exp(2\mathfrak{N}\mathfrak{B}_1) + \chi^c(\xi_2)^{-1/2} \exp(2\mathfrak{N}\mathfrak{B}_2)], \quad (4.14)$$

where

$$\chi = \mathfrak{M}_1'(\xi; \mathfrak{N}) \quad \text{and} \quad \chi^c = \mathfrak{M}_1^{c'}(\xi; \mathfrak{N}), \quad (4.15)$$

and we have only kept the first term in the asymptotic expansion of each integral. When $|\bar{\sigma}|$ is larger than the value of \mathfrak{M}_1 where $\mathfrak{M}_1 = \mathfrak{M}_1^c$, then the second term of (4.14) is smaller than $o(\exp(2\mathfrak{N}\alpha_2))$ and must be discarded. In (4.14), we may let \mathfrak{N} and \mathfrak{N} tend to infinity in any manner that we please and still obtain the same answer up to a factor which is independent of $\bar{\sigma}$.

When $\bar{\sigma}$ is very close to $\mathfrak{M}_1(0)$, the steepest-descent

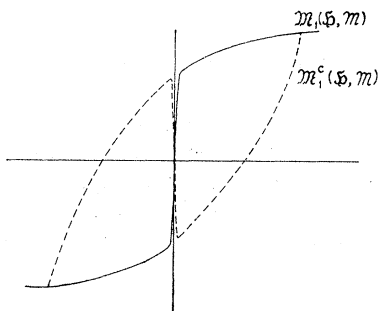


FIG. 2. Functions $\mathfrak{M}_1(\mathfrak{S}; \mathfrak{N})$ and $\mathfrak{M}_1^c(\mathfrak{S}; \mathfrak{N})$.

point ξ_1 is comparable in magnitude to \mathfrak{S}_0 and the previous evaluation breaks down because higher-order terms in the asymptotic expansions may no longer be ignored. For $|\bar{\sigma}| < \mathfrak{M}_1(0)$, there is still, nominally, a steepest-descent point on the first sheet of \mathfrak{F} , but the rapid variation of \mathfrak{F} near this point makes the point unimportant for an asymptotic expansion. In this region, we must deform the contour of integration of the first term of (4.11) through the imaginary-axis branch cuts to give an integral taken solely on the second sheet of \mathfrak{F} plus an additional integral whose path is from $-\mathfrak{S}_0$ to \mathfrak{S}_0 once on each sheet (Fig. 3). We may evaluate the integral on the second sheet and the second integral of (4.11) by steepest descents, where now both ξ_1 and ξ_2 ($|\xi_1| < |\xi_2|$) satisfy (4.13b). As seen from Fig. 2, (4.13b) has three solutions for $|\bar{\sigma}| < \mathfrak{M}_1(0)$, but the one closest to $\xi=0$ must be discarded. We thus obtain

$$\mathfrak{P}(\bar{\sigma}; \mathfrak{N}, \mathfrak{N}) = [1 + r_{\mathfrak{N}}(0)^{2\mathfrak{N}}]^{-1/2} (\beta/\pi\mathfrak{N})^{1/2} \times [\chi^c(\xi_1)^{-1/2} \exp(2\mathfrak{N}\mathfrak{B}_1) + \chi^c(\xi_2)^{-1/2} \exp(2\mathfrak{N}\mathfrak{B}_2)] + I_{\mathfrak{N}, \mathfrak{N}}(\bar{\sigma}), \quad (4.16)$$

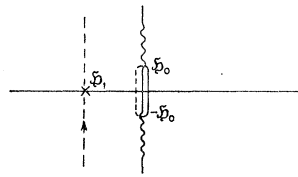


FIG. 3. Integration paths for $\mathfrak{P}(\bar{\sigma}; \mathfrak{N}, \mathfrak{N})$ when $|\bar{\sigma}| < \mathfrak{M}_1(0)$.

where

$$I_{\mathfrak{N}, \mathfrak{N}}(\bar{\sigma}) = \beta(2\pi)^{-1} \int_{-\mathfrak{S}_0}^{\mathfrak{S}_0} d\xi (1 - r_{\mathfrak{N}}^{2\mathfrak{N}}) [1 + r_{\mathfrak{N}}(0)^{2\mathfrak{N}}]^{-1} \times \exp\{-2\mathfrak{N}\beta[\xi\bar{\sigma} + \mathfrak{F}(\xi; \mathfrak{N})]\}. \quad (4.17)$$

Only $I_{\mathfrak{N}, \mathfrak{N}}$ depends on the order in which the \mathfrak{N} and $\mathfrak{N} \rightarrow \infty$ limits are taken. To analyze (4.17), define

$$h = -i2\mathfrak{N}\mathfrak{S}_0 = \mathfrak{N}\alpha(0)^{-2\mathfrak{N}} \{ [z_2(1+z_1)^2 - (1-z_1)^2] z_1 [1 - \alpha(0)^{-\mathfrak{N}\mathfrak{N}}] \}^{1/2}. \quad (4.18)$$

In IV, we analyzed the case $\mathfrak{N} \rightarrow \infty$ and then $\mathfrak{N} \rightarrow \infty$ which corresponds to $h=0$. For h not to tend to zero as \mathfrak{N} and $\mathfrak{N} \rightarrow \infty$, \mathfrak{N} must be exponentially larger than \mathfrak{N} . It is straightforward to evaluate (4.17) when h is small. This is done in Appendix B, and we obtain for $T < T_c$, $h \ll 1$, and $|\bar{\sigma}| < \mathfrak{M}_1(0)$

$$\mathfrak{P}(\bar{\sigma}; \mathfrak{N}, \mathfrak{N}) \sim \frac{1}{4} (\beta/\pi\mathfrak{N})^{1/2} [\chi^c(\xi_1)^{-1/2} \exp(2\mathfrak{N}\mathfrak{B}_1) + \chi^c(\xi_2)^{-1/2} \exp(2\mathfrak{N}\mathfrak{B}_2)] + \frac{1}{4} \mathfrak{M}_1(0) \times [1 - \alpha(0)^{-\mathfrak{N}\mathfrak{N}}]^{1/2} h [1 - \frac{1}{8} h^2 \bar{\sigma}^2 + O(h^4 \bar{\sigma}^2)]. \quad (4.19)$$

In this expression, there are two different sorts of

$\bar{\sigma}$ dependence: (a) Gaussian tails of magnitude $\exp(2\mathfrak{N}\mathfrak{B}_1)$ and $\exp(2\mathfrak{N}\mathfrak{B}_2)$ and (b) a polynomial of magnitude $2\mathfrak{N}\alpha(0)^{-2\mathfrak{N}}$. For different ways of taking the thermodynamic limit, the range of $\bar{\sigma}$ in which one term dominates the other is different. In particular, if $\mathfrak{N}\mathfrak{L} = K\mathfrak{N}$ and $\mathfrak{N} \rightarrow \infty$, $\mathfrak{P}(\bar{\sigma}; \mathfrak{N}\mathfrak{L}, \mathfrak{N})$ will be a constant for $|\bar{\sigma}| < \bar{\sigma}_0$, where $\bar{\sigma}_0$ is determined from

$$K \ln \alpha(0) + \mathfrak{B}_1(\bar{\sigma}_0) = 0. \tag{4.20}$$

In the opposite limit, $h \rightarrow \infty$, it is convenient to define

$$h' = 2\mathfrak{N}\alpha(0)^{-2\mathfrak{N}} = 2\mathfrak{N} [z_2(1+z_1)/(1-z_1)]^{-2\mathfrak{N}}. \tag{4.21}$$

From Appendix B we find that for $T < T_c$, $h' \rightarrow \infty$, and $|\sigma| < \mathfrak{M}_1(0)$

$$\begin{aligned} \mathfrak{P}(\bar{\sigma}; \mathfrak{N}\mathfrak{L}, \mathfrak{N}) \sim & (h'z_2/2\pi)^{1/2} (2\mathfrak{N})^{-1} \exp(-\frac{1}{2}h'\bar{\sigma}^2z_2) \\ & + \frac{1}{2}(\beta/\pi\mathfrak{N})^{1/2} [\chi^c(\xi_1)]^{1/2} \exp(2\mathfrak{N}\mathfrak{B}_1 + \chi^c(\xi_2) \\ & \times \exp(2\mathfrak{N}\mathfrak{B}_2)]. \end{aligned} \tag{4.22}$$

The first term is a Gaussian centered about $\bar{\sigma} = 0$ of width $z_2h'^{-1/2}$ and area 1. This is to be expected because $h' \rightarrow \infty$ means that the number of columns is exponentially larger than the number of rows, and the lattice for finite \mathfrak{N} and \mathfrak{N} looks extremely one-dimensional. There is clearly only one maximum in

$\mathfrak{P}(\bar{\sigma}; \mathfrak{N}\mathfrak{L}, \mathfrak{N})$ in this $h' \rightarrow \infty$ case. Therefore a metastable state can surely *not* exist when $\mathfrak{N} \rightarrow \infty$ and then $\mathfrak{N}\mathfrak{L} \rightarrow \infty$. There is a simple physical explanation for this. The factor $[z_2(1+z_1)/(1-z_1)]^{-2\mathfrak{N}}$ is the "boundary-tension"⁸ free-energy contribution to the partition function found by Onsager to arise in the rectangular Ising lattice when two regions of opposite magnetization have a boundary in common. This domain wall may occupy any of the $2\mathfrak{N}$ sites on the boundary. When h' is large, the gain in entropy that the lattice obtains by breaking up into domains outweighs the loss in energy, so that the lattice breaks up into many small regions of opposite magnetization, which means that there is no spontaneous magnetization.

For further interpretation of the meaning of the several pieces of $\mathfrak{P}(\bar{\sigma}; \mathfrak{N}\mathfrak{L}, \mathfrak{N})$, we confine ourselves to the $\mathfrak{N}\mathfrak{L} \rightarrow \infty$ ($h \rightarrow 0$) limit where (4.19) applies and the last term vanishes. As argued in IV, if we begin with a state in one of the two peaks of $\mathfrak{P}(\bar{\sigma})$, the system will surely stay in that state as long as the peak exists as a separate maximum. When $\mathfrak{M}_1^c(\mathfrak{S})$ is zero, however, we can no longer determine by looking at $\mathfrak{P}(\bar{\sigma}; \mathfrak{N}\mathfrak{L}, \mathfrak{N})$ alone whether the magnetization will fall to $\mathfrak{M}_1(\mathfrak{S})$ or continue to be $\mathfrak{M}_1^c(\mathfrak{S})$. To understand what happens, it is necessary to examine $\mathfrak{M}_J(\mathfrak{S})$, the magnetization in the J th row, given by (9.5) of IV as

$$\begin{aligned} \mathfrak{M}_J = & \pm (1-z^2)(1-z_2^2)^{J-1} \\ \det & \begin{bmatrix} \mathfrak{A}^{-1}(1, 0; 0, 0)_{DU} + (z^{-1}-z)^{-1} & \mathfrak{A}^{-1}(1, 0; 1, 0)_{DU} & \dots \mathfrak{A}^{-1}(1, 0; J-1, 0)_{DU} \\ \mathfrak{A}^{-1}(2, 0; 0, 0)_{DU} & \mathfrak{A}^{-1}(2, 0; 1, 0)_{DU} + (z_2^{-1}-z_2)^{-1} & \dots \mathfrak{A}^{-1}(2, 0; J-1, 0)_{DU} \\ \vdots & \vdots & \vdots \\ \mathfrak{A}^{-1}(J, 0; 0, 0)_{DU} & \mathfrak{A}^{-1}(J, 0; 1, 0)_{DU} & \dots \mathfrak{A}^{-1}(J, 0; J-1, 0)_{DU} + (z_2^{-1}-z_2)^{-1} \end{bmatrix}. \end{aligned} \tag{4.23}$$

The required inverse matrix elements have been computed in (7.7) of IV. All the matrix elements except the ones in the first column are analytic functions of \mathfrak{S} . The matrix elements in the first column are discontinuous at $\mathfrak{S} = 0$ and may be analytically continued as

$$\begin{aligned} \mathfrak{A}^{-1c}(j, 0; 0, 0)_{DU} - \mathfrak{A}^{-1}(j, 0; 0, 0)_{DU} & \\ & = (1-z^2)^{-1} [\mathfrak{M}_1^c(\mathfrak{S}) - \mathfrak{M}_1(\mathfrak{S})] \alpha(r)^{-j+1} \\ & = (1-z^2)^{-1} [\mathfrak{M}_1^c(\mathfrak{S}) - \mathfrak{M}_1(\mathfrak{S})] [(1+z_1)(z_2^2-z^2)z_2^{-1}(1-z_1)^{-1}(1-z^2)^{-1}]^{-j+1}. \end{aligned} \tag{4.24}$$

Therefore for any J

$$\begin{aligned} \mathfrak{M}_J^c(\mathfrak{S}) - \mathfrak{M}_J(\mathfrak{S}) = & \pm [\mathfrak{M}_1^c(\mathfrak{S}) - \mathfrak{M}_1(\mathfrak{S})] (1-z_2^2)^{J-1} \\ \det & \begin{bmatrix} 1 & \mathfrak{A}^{-1}(1, 0; 1, 0)_{DU} & \dots \mathfrak{A}^{-1}(1, 0; J-1, 0)_{DU} \\ \alpha(r)^{-1} & \mathfrak{A}^{-1}(2, 0; 1, 0)_{DU} + (z_2^{-1}-z_2)^{-1} & \dots \mathfrak{A}^{-1}(2, 0; J-1, 0)_{DU} \\ \vdots & \vdots & \vdots \\ \alpha(r)^{-J+1} & \mathfrak{A}^{-1}(J, 0; 1, 0)_{DU} & \dots \mathfrak{A}^{-1}(J, 0; J-1, 0)_{DU} + (z_2^{-1}-z_2)^{-1} \end{bmatrix}. \end{aligned} \tag{4.25}$$

⁸ L. Onsager, Phys. Rev. 65, 117 (1944).

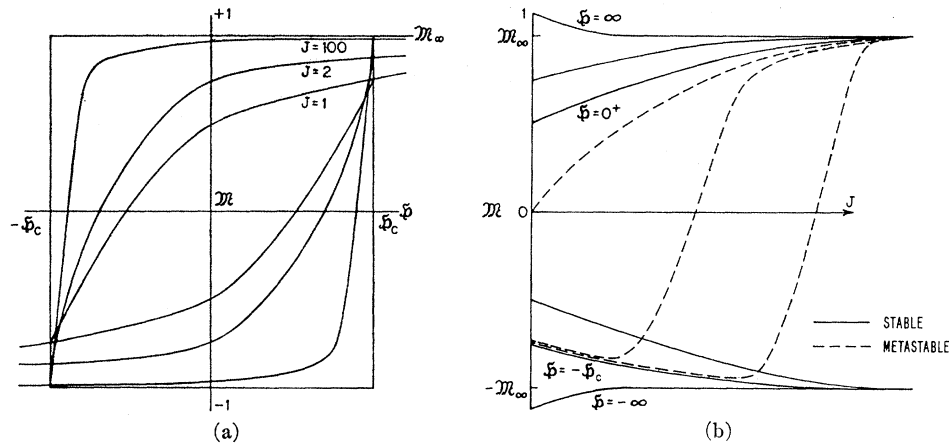


FIG. 4. Schematic behavior of $\mathcal{M}_J(\mathfrak{S})$ for $E_1 = E_2$ and $T/T_c = 0.9$. (a) $\mathcal{M}_J(\mathfrak{S})$ versus \mathfrak{S} for various J . (b) $\mathcal{M}_J(\mathfrak{S})$ versus J for various \mathfrak{S} . The metastable values between $\mathfrak{S} = 0^+$ and $-\mathfrak{S}_c$ are reached for positive values of \mathfrak{S} .

We do not propose to evaluate this explicitly, but merely note that, because the determinant is finite for all \mathfrak{S} , the value of \mathfrak{S}_c such that $\mathcal{M}_J^c(\mathfrak{S}_c) = \mathcal{M}_J(\mathfrak{S}_c)$ is the same for all J . The bulk magnetization can take on only the values $\pm M_\infty$ (the bulk magnetization of Yang⁹), so that the bulk spin must flip discontinuously from $+$ to $-M_\infty$ at $\mathfrak{S} = \mathfrak{S}_c$. This situation is pictured schematically in Fig. 4. Even though the magnetization in the first J rows may have passed beyond $\mathcal{M}_J^c(\mathfrak{S}) = 0$, there are still an infinite number of rows in which the magnetization has not yet passed $\mathcal{M}_J^c(\mathfrak{S}) = 0$. From this viewpoint, there is no reason to single out the passing of $\mathcal{M}_J^c(\mathfrak{S})$ through zero or the disappearance of a secondary maximum in $\mathfrak{P}(\bar{\sigma})$ as the criteria for the entire system to fall from $\mathcal{M}_J^c(\mathfrak{S})$ to $\mathcal{M}_J(\mathfrak{S})$. The analytic continuation of $\mathcal{M}_J(\mathfrak{S})$ will characterize the entire system as long as for each and every $\mathcal{M}_J(\mathfrak{S})$ the analytic continuation is possible. For finite J , $\mathcal{M}_J(\mathfrak{S})$ is continuable not only beyond $\mathfrak{S} = 0$, but even beyond $\mathfrak{S} = \pm \mathfrak{S}_c$. However, $M_\infty(\mathfrak{S})$ cannot be continued beyond $\pm \mathfrak{S}_c$, because we have seen that the bulk magnetization will be discontinuous at $\mathfrak{S} = \pm \mathfrak{S}_c$. Therefore, for the system as a whole, continuation past $\pm \mathfrak{S}_c$ is meaningless and in each row the transition from \mathcal{M}_J^c to \mathcal{M}_J occurs at the same value of \mathfrak{S} .

The previous discussion gives a natural interpretation to each of the first two terms of (4.14) and (4.19) taken separately. We are really observing a thermodynamic system which, for some values of \mathfrak{S} , has not one but two stable states. The fact that there are two distinct stable states is reflected in $\mathfrak{P}(\bar{\sigma})$ by the two terms, and $\mathfrak{P}(\bar{\sigma})$ is really the sum of two separate probabilities: the probability that the average boundary spin is $\bar{\sigma}$ and the bulk spin is $+M$ plus the probability that the average boundary spin is $\bar{\sigma}$ and the bulk spin is $-M$. Each of these probability functions is monomodal and previous discussions of secondary maxima fail to apply.

5. MISFIT BOND

We now turn to the question of the influence of boundary conditions on the boundary-spin probability

⁹ C. N. Yang, Phys. Rev. 85, 808 (1952).

functions. We study this by looking at the same half-plane lattice previously considered, but instead of imposing cyclic boundary conditions by joining the \mathfrak{N} th and the $-(\mathfrak{N}+1)$ th columns by bonds of energy E_1 , we join them by bonds of energy $-E_1$.

We shall compute the boundary-spin probability function $\mathfrak{P}_{(1)}(\bar{\sigma})$ for this lattice from (2.1). For this purpose, we need an expression for the partition function $Z_{(1)}$. The evaluation of the partition function in the presence of a boundary magnetic field may be reduced by exactly the same arguments as used in Sec. 2 of IV to the evaluation of an appropriate Pfaffian as

$$Z_{(1)} = \frac{1}{2} (2 \cosh \beta E_1)^{4\mathfrak{N}\mathfrak{N}} (\cosh \beta E_2)^{2\mathfrak{N}(2\mathfrak{N}-1)} (\cosh \beta \mathfrak{S})^{2\mathfrak{N}} \times Pf \mathfrak{A}_{(1)}, \quad (5.1)$$

where $\mathfrak{A}_{(1)}$ is the matrix whose Pfaffian counts the lattice of Fig. 5(a). The elements of $\mathfrak{A}_{(1)}$ are exactly the same as those of \mathfrak{A} given in (2.6) of IV, except that (2.6d) is replaced with

$$\mathfrak{A}_{(1)}(0, \mathfrak{N}; 0, -\mathfrak{N}+1) = -\mathfrak{A}_{(1)}^T(0, -\mathfrak{N}+1; 0, \mathfrak{N}) = -\mathfrak{A}_{(1)}(0, 0; 0, 1) \quad (5.2)$$

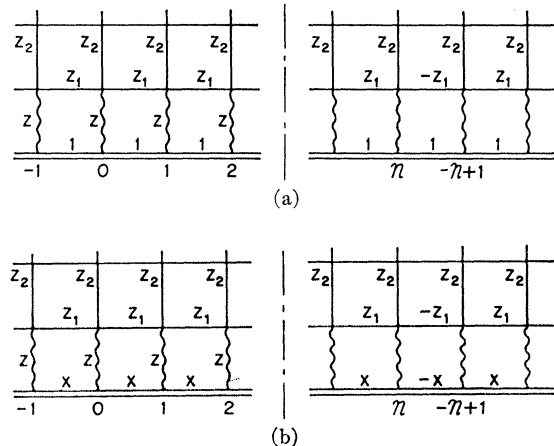


FIG. 5. (a) Misfit bond lattice counted by $\mathfrak{A}_{(1)}$. (b) Comparison lattice counted by \mathfrak{A} .

and

$$\mathfrak{A}_{(1)}(j, \mathfrak{N}; j, -\mathfrak{N}+1) = -\mathfrak{A}_{(1)}^T(j, -\mathfrak{N}+1; j, \mathfrak{N}) = \mathfrak{A}_{(1)}(j, 0; j, 1) \tag{5.3}$$

for $1 \leq j \leq 2\mathfrak{N}$.

The matrix $\mathfrak{A}_{(1)}$ is neither cyclic nor near cyclic, so we cannot immediately evaluate its Pfaffian. However, its Pfaffian may be evaluated by relating it to the Pfaffian of the cyclic matrix \mathfrak{A}_x which counts the weighted polygons drawn on the lattice of Fig. 5(b). The elements of \mathfrak{A}_x are the same as those of $\mathfrak{A}_{(1)}$, except for elements connecting sites in the zeroth row, where we have

$$\mathfrak{A}_x(0, k; 0, k+1) = -\mathfrak{A}_x^T(0, k+1; 0, k)$$

$$= \begin{matrix} & R & L & U & D \\ \begin{matrix} R \\ L \\ U \\ D \end{matrix} & \begin{bmatrix} 0 & x & 0 & 0 \\ 0 & 0 & 0 & 0 \\ 0 & 0 & 0 & 0 \\ 0 & 0 & 0 & 0 \end{bmatrix} & & & \end{matrix}, \tag{5.4}$$

for $-\mathfrak{N}+1 \leq k \leq \mathfrak{N}-1$, and

$$\mathfrak{A}_x(0, \mathfrak{N}; 0, -\mathfrak{N}+1) = -\mathfrak{A}_x^T(0, -\mathfrak{N}+1; 0, \mathfrak{N}) = \mathfrak{A}_x(0, 0; 0, 1). \tag{5.5}$$

When $x=1$, $Pf\mathfrak{A}_x=0$, because for every diagram that can be drawn on the lattice of Fig. 5(b) there is a complementary diagram which differs from the original only in using (omitting) all the bonds in the zeroth row which are omitted (used) in the original. This complementary diagram has the same magnitude as the original one, but opposite sign.

Consider all terms that may appear in the expansion of $Pf\mathfrak{A}_{(1)}$ that correspond to the diagrams drawn on Fig. 5(a) that differ (a) only in the two ways in which the sites in the zeroth row may be connected together and (b) by translation. If one such diagram has l bonds in the zeroth row, the complementary diagram has $2\mathfrak{N}-l$ bonds in the zeroth row. Denote the value of such a diagram when it is in a position where none of the l zero-row bonds is between \mathfrak{N} and $-\mathfrak{N}+1$ by d . Then the sum of this class of diagrams is

$$2(2\mathfrak{N}-l)d - 2ld = 4(\mathfrak{N}-l)d. \tag{5.6}$$

Now consider the same diagrams drawn on the lattice of Fig. 5(b) that now contribute to $Pf\mathfrak{A}_x$. The sum of

this same class of diagrams is now

$$(2\mathfrak{N}-l)(x^l - x^{2\mathfrak{N}-l})d + l(x^l - x^{2\mathfrak{N}-l})d = 2\mathfrak{N}x^l(1 - x^{2(\mathfrak{N}-l)})d. \tag{5.7}$$

If we sum (5.6) and (5.7) over all possible d , we reconstitute the Pfaffians of $\mathfrak{A}_{(1)}$ and \mathfrak{A}_x , respectively. From (5.7) we see that

$$\lim_{x \rightarrow 1} Pf\mathfrak{A}_x = 0$$

as expected, but also that we have the identity

$$\partial Pf\mathfrak{A}_x / \partial x |_{x=1} = -\mathfrak{N} Pf\mathfrak{A}_{(1)}. \tag{5.8}$$

Therefore

$$(\partial^2 / \partial x^2) \det\mathfrak{A}_x |_{x=1} = 2\mathfrak{N}^2 \det\mathfrak{A}_{(1)}. \tag{5.9}$$

We may evaluate $\det\mathfrak{A}_x$ in a manner analogous to the evaluation of $\det\mathfrak{A}$ in Sec. 3 of IV. Since \mathfrak{A}_x is a cyclic matrix,

$$\det\mathfrak{A}_x = \prod_{\phi} \det\mathfrak{B}_x(\phi), \tag{5.10}$$

where the product is over the $2\mathfrak{N}$ roots of 1;

$$\phi = n\pi / \mathfrak{N}, \tag{5.11}$$

where $n=0, 1, \dots, 2\mathfrak{N}-1$; and $\mathfrak{B}_x(\phi)$ is the $4(2\mathfrak{N}+1) \times 4(2\mathfrak{N}+1)$ matrix defined as in (3.3) of IV, with θ replaced with ϕ and B_{00} replaced with

$$\mathfrak{B}_{x0,0}(\phi) = \begin{bmatrix} 0 & 1+xe^{i\phi} & -1 & -1 \\ -1-xe^{-i\phi} & 0 & 1 & -1 \\ 1 & 1 & 0 & 1 \\ 1 & 1 & -1 & 0 \end{bmatrix}. \tag{5.12}$$

Defining

$$c_x = 2ix \sin\phi |1+xe^{i\phi}|^{-2} \tag{5.13a}$$

and

$$d_x = (1-x^2) |1+xe^{i\phi}|^{-2}, \tag{5.13b}$$

and following the procedure of IV, we find

$$\det\mathfrak{A}_x = \prod_{\phi} [|1+xe^{i\phi}|^2 |1+z_1e^{i\phi}|^{4\mathfrak{N}} \det\mathfrak{C}_x(\phi)], \tag{5.14}$$

where the elements of $\mathfrak{C}_x(\phi)$ are identical with those of $\mathfrak{C}(\theta)$ of (3.8) of IV, except that

$$\mathfrak{C}_{x0,0}(\phi) = \begin{bmatrix} -c_x & d_x \\ -d_x & c_x \end{bmatrix}. \tag{5.15}$$

Evaluating $\det\mathfrak{C}_x(\phi)$ as in IV, we obtain

$$\det\mathfrak{A}_x = \prod_{\phi} |1-xe^{i\phi}|^2 |1+z_1e^{i\phi}|^{4\mathfrak{N}\lambda 2\mathfrak{N}} \{ v^2 [1 - iz^2 z_2^{-1} c_x^{-1} (1 - d_x^2 c_x^{-2})^{-1} v' / v] + \alpha^{-4\mathfrak{N}} v'^2 [1 + iz^2 z_2^{-1} c_x^{-1} (1 - d_x^2 c_x^{-2})^{-1} v / v'] \}. \tag{5.16}$$

Since

$$\prod_{\phi} |1-xe^{i\phi}|^2 = (1-x^{2\mathfrak{N}})^2, \tag{5.17}$$

we may use (5.16) and (5.9) to evaluate (5.1) as

$$Z_{(1)}^2 = (2 \cosh \beta E_1)^{8\mathfrak{N}\mathfrak{N}} (\cosh \beta E_2)^{4\mathfrak{N}(2\mathfrak{N}-1)} (\cosh \beta \mathfrak{G})^{4\mathfrak{N}} \times \prod_{\phi} |1 + z_1 e^{i\phi}|^{4\mathfrak{N}\lambda^{2\mathfrak{N}}} \lim_{z \rightarrow 1} \prod_{\phi} \{v^2 [1 - iz^2 z_2^{-1} c_x^{-1} (1 - d_x^2 c_x^{-2})^{-1} v'/v] + \alpha^{-4\mathfrak{N}} v'^2 [1 + iz^2 z_2^{-1} c_x^{-1} (1 - d_x^2 c_x^{-2})^{-1} v/v']\}. \quad (5.18)$$

The $\phi=0$ term in this last product must be treated separately. For $T > T_c$ we have

$$Z_{(1)}^2 = (2 \cosh \beta E_1)^{8\mathfrak{N}\mathfrak{N}} (\cosh \beta E_2)^{4\mathfrak{N}(2\mathfrak{N}-1)} (\cosh \beta \mathfrak{G})^{4\mathfrak{N}} \prod_{\phi} |1 + z_1 e^{i\phi}|^{4\mathfrak{N}\lambda^{2\mathfrak{N}}} \prod'_{\phi} [v^2 (1 - iz^2 z_2^{-1} c^{-1} v'/v) + \alpha^{-4\mathfrak{N}} v'^2 (1 + iz^2 z_2^{-1} c^{-1} v/v')], \quad (5.19a)$$

while for $T < T_c$

$$Z_{(1)}^2 = (2 \cosh \beta E_1)^{8\mathfrak{N}\mathfrak{N}} (\cosh \beta E_2)^{4\mathfrak{N}(2\mathfrak{N}-1)} (\cosh \beta \mathfrak{G})^{4\mathfrak{N}} \alpha(0)^{-4\mathfrak{N}} \prod_{\phi} |1 + z_1 e^{i\phi}|^{4\mathfrak{N}\lambda^{2\mathfrak{N}}} \prod'_{\phi} [v^2 (1 - iz^2 z_2^{-1} c^{-1} v'/v) + \alpha^{-4\mathfrak{N}} v'^2 (1 + iz^2 z_2^{-1} c^{-1} v/v')], \quad (5.19b)$$

where \prod'_{ϕ} means to take the product over all $\phi \neq 0$ satisfying (5.11) and we have used the facts that for $T > T_c$, $v(0) = 1$, and as $\phi \rightarrow 0$,

$$v'(\phi) \rightarrow 2z_1 z_2 \phi [z_2^2 (1 + z_1)^2 - (1 - z_1)^2]^{-1}, \quad (5.20a)$$

while for $T < T_c$, $v'(0) = 1$, and as $\phi \rightarrow 0$,

$$v(\phi) \rightarrow -2z_1 z_2 \phi [z_2^2 (1 + z_1)^2 - (1 - z_1)^2]^{-1}. \quad (5.20b)$$

To convert (5.19) into an integral, we must reinstate the $\phi=0$ term into the product and use the Poisson-sum formula appropriate to the $2\mathfrak{N}$ roots of 1,

$$\sum_{n=0}^{2\mathfrak{N}-1} \delta(\phi - n\pi/2\mathfrak{N}) = 2\mathfrak{N}\pi^{-1} \sum_{m=-\infty}^{\infty} e^{2\mathfrak{N}mi\phi}. \quad (5.21)$$

The integrals are then exactly the same as those analyzed in Sec. 2, with the exception of the omission of $(-1)^m$. A completely analogous calculation, therefore, gives for $T > T_c$

$$Z_{(1)}(\mathfrak{G})/Z_{(1)}(0) = \{1 + 4z^2 z_1 [1 - \alpha(0)^{-4\mathfrak{N}}] [(1 - z_1)^2 - z_2^2 (1 + z_1)^2]^{-1/2} \times (\cosh \beta \mathfrak{G})^{2\mathfrak{N}} \exp\{-2\mathfrak{N}\beta \mathfrak{F}(\mathfrak{G}; \mathfrak{N}) [1 + o(\alpha_2^{-2\mathfrak{N}})]\} \quad (5.22a)$$

and for $T < T_c$

$$Z_{(1)}(\mathfrak{G})/Z_{(1)}(0) = \{1 + 4z^2 z_1 [\alpha(0)^{4\mathfrak{N}} - 1] [z_2^2 (1 + z_1)^2 - (1 - z_1)^2]^{-1/2} \times (\cosh \beta \mathfrak{G})^{2\mathfrak{N}} (1 - r_{\mathfrak{N}}^{2\mathfrak{N}}) [1 - r_{\mathfrak{N}}(0)^{2\mathfrak{N}}]^{-1} \exp\{-2\mathfrak{N}\beta \mathfrak{F}(\mathfrak{G}; \mathfrak{N}) [1 + o(\alpha_2^{2\mathfrak{N}})]\}, \quad (5.22b)$$

where

$$Z_{(1)}^2(0) = (2 \cosh \beta E_1)^{8\mathfrak{N}\mathfrak{N}} (\cosh \beta E_2)^{4\mathfrak{N}(2\mathfrak{N}-1)} \prod_{\phi} |1 + z_1 e^{i\phi}|^{4\mathfrak{N}\lambda^{2\mathfrak{N}}} v^2 [1 + \alpha^{-4\mathfrak{N}} (v'/v)^2]. \quad (5.23)$$

Expression (5.22a) is exactly the same as the partition function above T_c when there is no misfit bond, with the exception of the first factor. This extra factor is easily interpreted as the decrease in free energy caused by the boundary magnetic field forcing spins on opposite sides of the misfit seam to point in the same direction. When $T \rightarrow T_c+$, this factor becomes very small, on the order of $(2\mathfrak{N})^{-1}$. This is because very near T_c the correlation length is very large and the boundary magnetic field is able to line spins up across the seam at depths into the bulk on the order of $2\mathfrak{N}$.

To show that the misfit bonds have destroyed the bimodal character of $\mathfrak{F}(\bar{\sigma})$, we consider the $\mathfrak{N} \rightarrow \infty$ limit of (5.22b) and obtain

$$\lim_{\mathfrak{N} \rightarrow \infty} [Z_{(1)}(\mathfrak{G})/Z_{(1)}(0)] = (1 - r^{2\mathfrak{N}}) [4\mathfrak{N}(z^2)^{1/2} \mathfrak{M}_1(0)]^{-1} \exp[-2\mathfrak{N}\beta \mathfrak{F}(\mathfrak{G})], \quad (5.24)$$

where $\mathfrak{F}(\mathfrak{G})$ and $(z^2)^{1/2}$ are analytic in the \mathfrak{G} plane cut along the entire imaginary \mathfrak{G} axis, because we have let $\mathfrak{N} \rightarrow \infty$ and $(z^2)^{1/2}$ is positive when z is real. Similarly, the \mathfrak{G} plane in which r is analytic is cut along the imaginary axis. The second sheet of all of these functions may be obtained by continuing through this cut as we did in (4.8) and (4.9) for finite \mathfrak{N} . If we use those expressions for r^c and \mathfrak{F}^c in (5.24), we find that, as expected, $Z_{(1)}(\mathfrak{G})$ does not have a branch cut on the imaginary axis.

We now use (5.24) in (2.1) to obtain

$$\mathfrak{P}_{(1)}(\bar{\sigma}) = \beta(2\pi i)^{-1} \int_{-i\pi/\beta}^{i\pi/\beta} d\xi (1 - \tau^{2\mathfrak{N}}) [4\mathfrak{N}z\mathfrak{M}_1(0)]^{-1} \exp\{-2\mathfrak{N}\beta[\mathfrak{F}(\xi) + \bar{\sigma}\xi]\}, \quad (5.25)$$

where the integration path has been deformed slightly to the right of the imaginary axis. We evaluate (5.25) by steepest descents, where, as before, the terms of $O(1)$ and $O(\tau^{2\mathfrak{N}})$ have different steepest-descent points and must be evaluated separately. But once this separation is made, we see that each separate term has a pole at $\xi=0$, so that when the steepest-descent point occurs at negative ξ , we pick up an extra contribution from this pole. When $\bar{\sigma}$ is enough larger than $\mathfrak{M}_1(0)$ so that the steepest-descent points are away from $\xi=0$, we have

$$\mathfrak{P}_{(1)}(\bar{\sigma}) = [8\mathfrak{N}\mathfrak{M}_1(0)]^{-1} (\beta/\mathfrak{N}\pi)^{1/2} [\chi(\xi_1)^{-1/2} \coth\beta\xi_1 \exp(2\mathfrak{N}\mathfrak{B}_1) - \chi^c(\xi_2)^{-1/2} \coth\beta\xi_2 \exp(2\mathfrak{N}\mathfrak{B}_2)], \quad (5.26)$$

with ξ_1 and ξ_2 given by (4.12). When $0 < |\bar{\sigma}| < \mathfrak{M}_1(0)$,

$$\mathfrak{P}_{(1)}(\bar{\sigma}) = [2\mathfrak{N}\mathfrak{M}_1(0)]^{-1} + [8\mathfrak{N}\mathfrak{M}_1(0)]^{-1} (\beta/\pi\mathfrak{N})^{1/2} \times [\chi^c(\xi_1)^{-1/2} \coth\beta\xi_1 \exp(2\mathfrak{N}\mathfrak{B}_1) - \chi^c(\xi_2)^{-1/2} \coth\beta\xi_2 \exp(2\mathfrak{N}\mathfrak{B}_2)]. \quad (5.27)$$

When $\mathfrak{N} \rightarrow \infty$, this expression is dominated by a constant. This flatness of $\mathfrak{P}_{(1)}(\bar{\sigma})$ has an obvious physical interpretation. When $\mathfrak{S}=0$, the $-E_1$ bonds force the lattice to break up into two domains of opposite spin. One wall between these domains must be the column of $-E_1$ bonds, but the other wall may be anywhere. Therefore the surface magnetization is uniformly distributed between $\pm\mathfrak{M}_1(0)$, depending on where the other domain wall may be. This physical picture applies to the bulk as well, and we expect that the bulk probability functions as well as $\mathfrak{P}_{(1)}$ are flat between $\pm M$. To prove this, one needs to consider the behavior of the correlation functions when the separation becomes large. For the boundary spin-spin correlation, it is straightforward to show from IV that for large k

$$\langle \sigma_{10}\sigma_{1k} \rangle \rightarrow \mathfrak{M}_1^2(\mathfrak{N} - |k|)/\mathfrak{N} + O(\alpha_2^{|k|}). \quad (5.28)$$

For completeness, it remains only to evaluate (5.25) when $\bar{\sigma}$ is very close to $\mathfrak{M}_1(0)$. This is easily done in terms of the complementary error function, and we

obtain

$$\mathfrak{P}_{(1)}(\bar{\sigma}) \sim [2\mathfrak{N}\mathfrak{M}_1(0)]^{-1} \pi^{-1/2} \times \text{Erfc}\{[\bar{\sigma} - \mathfrak{M}_1(0)](\mathfrak{N}\beta/\chi)^{1/2}\}. \quad (5.29)$$

6. NUMERICAL CALCULATIONS

The expression for $\mathfrak{M}_1(\mathfrak{S})$, (5.1) of IV, is in the form of an integral which, in general, cannot be expressed in terms of elementary functions. To obtain a more complete understanding of the magnetic properties of the boundary, we have numerically computed \mathfrak{M}_1 and χ on an IBM 7044, using a Simpson's-rule integration. We have, in particular, studied these functions near T_c , where they fail to be analytic. In IV, we obtained the behavior of \mathfrak{M} and χ near $\mathfrak{S}=0$ and $T=T_c$ for $E_1>0$. It is also necessary, however, to determine the behavior near T_c for $E_1>0$ with \mathfrak{S} away from zero and for $E_1<0$. This can easily be done using the devices of analytic continuation and Pochhammer's contour of Sec. 4 of IV. In this way, we obtain for $E_1>0$, \mathfrak{S} away from zero, and $T \sim T_c$

$$\mathfrak{M}_1(\mathfrak{S}) = \text{Taylor series in } \tau_2 + [z^{-3}\pi^{-1} |z_2| (1-z^2)\tau_2^2 + O(\tau_2^3)] \ln |\tau_2|, \quad (6.1)$$

where

$$\tau_2 = (1-\alpha_2)/(1+\alpha_2) \quad (6.2)$$

and the other notations of IV have been recalled in Ref. 6. For $E_1<0$ and \mathfrak{S} arbitrary

$$\mathfrak{M}_1(\mathfrak{S}) = \text{Taylor series in } \tau_2^{-1} + [|z_2|^{-1}\pi^{-1}(1-z^2)z\tau_2^{-2} + O(\tau_2^{-3})] \ln |\tau_2^{-1}|. \quad (6.3)$$

In both cases, the Taylor series above T_c are the same as those below T_c . We clearly see that \mathfrak{M}_1 and χ are *not* analytic functions of T at $T=T_c$ for \mathfrak{S} away from zero, because the second derivative with respect to T

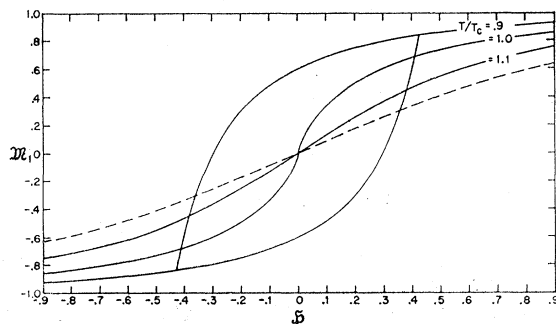


FIG. 6. \mathfrak{M}_1 versus \mathfrak{S} for $E_1=E_2=1$ (ferromagnetic) at various T/T_c . The dotted line is the one-dimensional ($E_1=1$, $E_2=0$) magnetization at the same temperature as $T/T_c=1.1$.

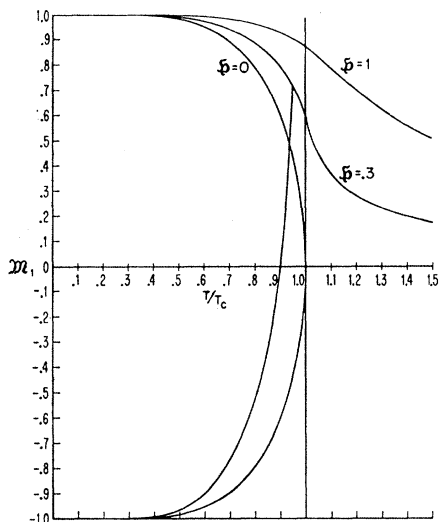


FIG. 7. Boundary magnetization versus temperature for $E_1=E_2=1$ at various values of \mathfrak{S} .

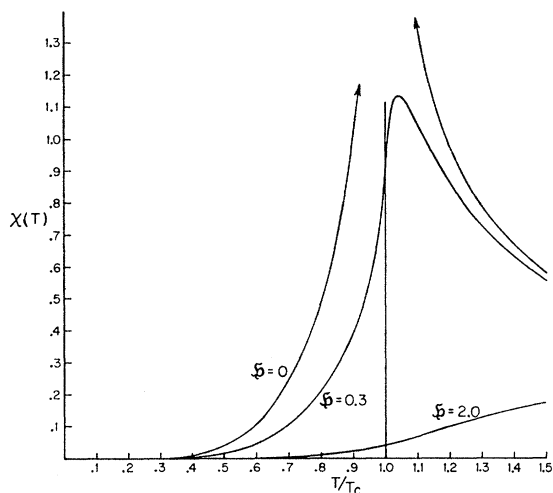


FIG. 8. Boundary susceptibility versus temperature for $E_1=E_2=1$ at various values of \mathfrak{S} .

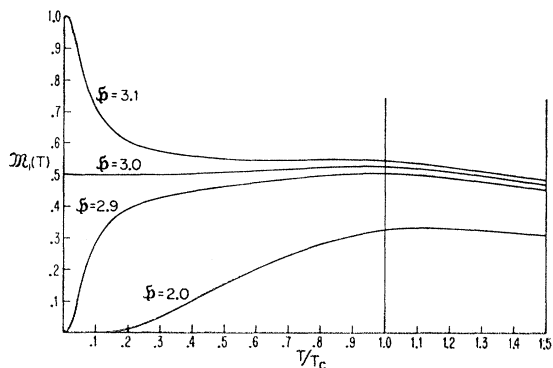


FIG. 9. Boundary magnetization versus temperature for $E_1=-E_2=-1$ (antiferromagnetic) at various values of \mathfrak{S} .

does not exist there. However, this nonanalytic behavior at T_c will not prevent \mathfrak{M}_1 and χ from looking perfectly smooth at T_c .

In Fig. 6, we plot \mathfrak{M}_1 versus \mathfrak{S} for $E_1=E_2=1$ (all energies on the scale $k=1$) for several T . For comparison, we also plot the one-dimensional case $E_1=1, E_2=0$ at $T=2.498$, which corresponds to $T/T_c=1.1$ when $E_1=E_2$. In Fig. 7, we plot \mathfrak{M}_1 versus T/T_c for $E_1=E_2=1$ at $\mathfrak{S}=0, 0.3$, and 1 , and we particularly note the smooth appearance of the latter two curves at $T=T_c$. In Fig. 8, we plot χ versus T and note, in particular, how the logarithmic divergence in χ for $\mathfrak{S}=0$ at $T=T_c$ becomes a maximum which occurs at $T>T_c$ for $\mathfrak{S}\neq 0$. In Fig. 9, we show \mathfrak{M}_1 in the antiferromagnetic ($E_1=-E_2=-1$) case versus T , and finally, in Fig. 10, we plot χ in the antiferromagnetic case versus T . In this last case, the shallow maximum which occurs slightly above T_c at $\mathfrak{S}=0$ moves below

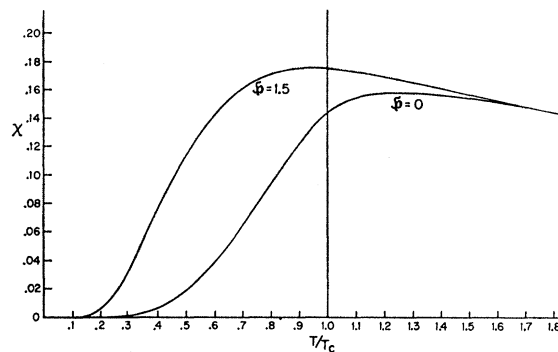


FIG. 10. Boundary susceptibility versus temperature $E_1=-E_2=-1$ (antiferromagnetic) at various values of \mathfrak{S} .

T_c as \mathfrak{S} is increased and will become a divergence at $T=0$ when $\mathfrak{S}=3$. All of these curves look perfectly smooth at $T=T_c$, even though they have infinite second derivatives there.

ACKNOWLEDGMENT

We are greatly indebted to Professor C. N. Yang for most helpful discussions.

APPENDIX A

To evaluate (4.2), we must first locate the singularities of the integrand of (4.2) near the unit circle. This integrand is singular either when (4.4) holds or when

$$1 + (v'/v)^2 \alpha^{-4\mathfrak{M}} = 0. \tag{A1}$$

When \mathfrak{S} is real and $T>T_c$, (4.4) has no solutions near $|e^{i\theta}|=1$, so that we confine our attention to $T<T_c$. Here the only solutions to (4.4) near $|e^{i\theta}|=1$ are $r_{3\pi}(\mathfrak{S})$ and $r_{3\pi}(\mathfrak{S})^{-1}$. Similarly, the only values of $e^{i\theta}$ near $|e^{i\theta}|=1$ when (A1) holds are $r_{3\pi}(0)$ and $r_{3\pi}(0)^{-1}$. When θ is near zero and $T<T_c$, we find from (3.20) of IV that

$$v'/v \sim -[z_2^2(1+z_1)^2 - (1-z_1)^2](2z_2z_1\theta)^{-1}. \tag{A2}$$

Using (A2) in (4.4), we find that for $r_{3\mathfrak{N}}$ near 1

$$(r_{3\mathfrak{N}} - 1)^2 \sim z_1^{-1} z_2^{-2} [z_2^2 (1 + z_1)^2 - (1 - z_1)^2] \\ \times \{z^2 [1 - \alpha(0)^{-43\mathfrak{N}}] + \frac{1}{4} z_1^{-1} \alpha(0)^{-43\mathfrak{N}} \\ \times [z_2^2 (1 + z_1)^2 - (1 - z_1)^2]\}, \quad (\text{A3})$$

so that for \mathfrak{S} near \mathfrak{S}_0

$$r_{3\mathfrak{N}}(\mathfrak{S}) \sim 1 - 2\mathfrak{M}_1(0) [1 - \alpha(0)^{-43\mathfrak{N}}]^{1/2} (z^2 - z_0^2)^{1/2}. \quad (\text{A4})$$

The branch points at $\pm\mathfrak{S}_0$ are square-root branch points, and in the region near $\pm\mathfrak{S}_0$ the only important difference between $r_{3\mathfrak{N}}$ and r of (5.11) of IV is that $(z^2)^{1/2}$ is replaced with $(z^2 - z_0^2)^{1/2}$. Equation (4.9) is obtained immediately by continuing $r_{3\mathfrak{N}}(\mathfrak{S})$ through the cut on the imaginary axis.

These considerations show that $\mathfrak{F}(\mathfrak{S}; \mathfrak{N})$ of (4.3) is an analytic function of \mathfrak{S} in the cut \mathfrak{S} plane, is real for \mathfrak{S} real, and is an even function of \mathfrak{S} . To obtain the analytic continuation of $\mathfrak{F}(\mathfrak{S}; \mathfrak{N})$, first consider $0 < \mathfrak{S} < |\mathfrak{S}_0|$. When we continue \mathfrak{S} around \mathfrak{S}_0 , $r_{3\mathfrak{N}}(\mathfrak{S}) \rightarrow r_{3\mathfrak{N}}^c(\mathfrak{S}) = r_{3\mathfrak{N}}^{-1}(\mathfrak{S})$, and the contour of integration is deformed as in Fig. 11. Therefore, with $\zeta = e^{i\theta}$,

$$\mathfrak{F}^c(\mathfrak{S}; \mathfrak{N}) - \mathfrak{F}(\mathfrak{S}; \mathfrak{N}) = -\beta^{-1} (4\pi i)^{-1} \int_c d\zeta \zeta^{-1} \\ \times \ln \{ [1 + \alpha^{-43\mathfrak{N}} (v'/v)^2]^{-1} [(1 - iz^2 z_2^{-1} c^{-1} v'/v) \\ + \alpha^{-43\mathfrak{N}} (v'/v)^2 (1 + iz^2 z_2^{-1} c^{-1} v'/v)] \} \\ = \frac{1}{2} \beta^{-1} \int_{r_{3\mathfrak{N}}^{-1}}^{r_{3\mathfrak{N}}} d\zeta \zeta^{-1} = -\beta^{-1} \ln r_{3\mathfrak{N}}. \quad (\text{A5})$$

This result may be analytically continued to all \mathfrak{S} and establishes (4.8).

These considerations suffice to understand the $m=0$ term in (4.2). To analyze the contribution for $m>0$ at $T < T_c$, it is sufficient to deform the contour to go

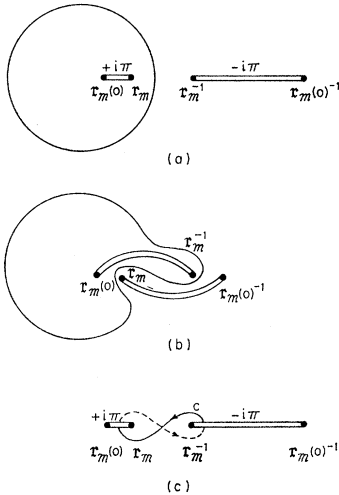


FIG. 11. Integration contour for (a) $\mathfrak{F}(\mathfrak{S}, \mathfrak{N})$, (b) $\mathfrak{F}^c(\mathfrak{S}, \mathfrak{N})$, and (c) $\mathfrak{F}^c(\mathfrak{S}, \mathfrak{N}) - \mathfrak{F}(\mathfrak{S}, \mathfrak{N})$ in the $e^{i\theta} = \zeta$ plane. Only cuts at $r_{3\mathfrak{N}}$ and $r_{3\mathfrak{N}}(0)$ are shown. The definition of the imaginary part of the logarithm is shown.

around the logarithmic branch cut from $r_{3\mathfrak{N}}(\mathfrak{S})$ to $r_{3\mathfrak{N}}(0)$ and neglect the contributions from the other branch cuts (for $m < 0$, first send $\theta \rightarrow -\theta$). Then

$$(2\pi)^{-1} \int_{-\pi}^{\pi} d\theta [-\exp(23\mathfrak{N}i\theta)]^m \ln \{ [1 + \alpha^{-43\mathfrak{N}} (v'/v)^2]^{-1} \\ \times [(i - iz^2 z_2^{-1} c^{-1} v'/v) + \alpha^{-43\mathfrak{N}} (v'/v)^2 (1 + iz^2 z_2^{-1} c^{-1} v'/v)] \} \\ = (-1)^m (23\mathfrak{N} | m |)^{-1} [r_{3\mathfrak{N}}(0)^{23\mathfrak{N} | m |} - r_{3\mathfrak{N}}^{23\mathfrak{N} | m |}] \\ + O(\exp(-3\mathfrak{N} | m | \alpha_2^{-1})). \quad (\text{A6})$$

Using

$$\sum_{m=1}^{\infty} (-1)^m (2m3\mathfrak{N})^{-1} x^{23\mathfrak{N}m} = -(23\mathfrak{N})^{-1} \ln(1 + x^{23\mathfrak{N}}), \quad (\text{A7})$$

we obtain (4.10).

APPENDIX B

To derive approximations to $I_{3\mathfrak{N}, \mathfrak{N}}$ of (4.17), we use the fact that, because $|\xi| < |\mathfrak{S}_0| \sim 0$, we have $|r_{3\mathfrak{N}}(\xi)| < |r_{3\mathfrak{N}}(0)|$ and may approximate

$$\mathfrak{F}(\xi; \mathfrak{N}) \sim \frac{1}{2} \beta^{-1} \ln [r_{3\mathfrak{N}}/r_{3\mathfrak{N}}(0)] + O(\xi^2) \quad (\text{B1})$$

to obtain

$$I_{3\mathfrak{N}, \mathfrak{N}}(\bar{\sigma}) \sim \beta (2\pi i)^{-1} \int_{-\mathfrak{S}_0}^{\mathfrak{S}_0} d\xi (r_{3\mathfrak{N}}^{-3\mathfrak{N}} - r_{3\mathfrak{N}}^{3\mathfrak{N}}) \\ \times [r_{3\mathfrak{N}}(0)^{-3\mathfrak{N}} + r_{3\mathfrak{N}}(0)^{3\mathfrak{N}}]^{-1} \exp(-23\mathfrak{N}\beta\bar{\sigma}). \quad (\text{B2})$$

When $h \ll 1$, we may change variables to $\zeta = \xi/\mathfrak{S}_0$ and use (A4) to obtain

$$I_{3\mathfrak{N}, \mathfrak{N}}(\bar{\sigma}) \sim h \mathfrak{M}_1(0) [1 - \alpha(0)^{-43\mathfrak{N}}]^{1/2} \\ \times (2\pi)^{-1} \int_{-1}^1 d\zeta (1 - \zeta^2)^{1/2} \exp(ih\bar{\sigma}\zeta) \\ = \frac{1}{2} \mathfrak{M}_1(0) [1 - \alpha(0)^{-43\mathfrak{N}}]^{1/2} \bar{\sigma}^{-1} J_1(h\bar{\sigma}), \quad (\text{B3})$$

where J_1 is the Bessel function of the first kind. From this we obtain (4.19).

In the opposite limit, $h' \rightarrow \infty$, $3\mathfrak{N}$ is so much larger than \mathfrak{N} that $r_{3\mathfrak{N}}(0)^{3\mathfrak{N}} \sim 0$ and, except for $\xi = \mathfrak{S}_0$, $r_{3\mathfrak{N}}^{-3\mathfrak{N}} - r_{3\mathfrak{N}}^{3\mathfrak{N}} \sim r_{3\mathfrak{N}}^{-3\mathfrak{N}}$. We may therefore approximate $I_{3\mathfrak{N}, \mathfrak{N}}$ by

$$I_{3\mathfrak{N}, \mathfrak{N}}(\bar{\sigma}) \sim \beta (2\pi i)^{-1} \int_{-i\epsilon}^{i\epsilon} d\xi \\ \times [r_{3\mathfrak{N}}(0)/r_{3\mathfrak{N}}]^{3\mathfrak{N}} \exp(-23\mathfrak{N}\bar{\sigma}\beta\xi), \quad (\text{B4})$$

where ϵ is some small real number less than $|\mathfrak{S}_0|$. We may now approximate $r_{3\mathfrak{N}}(\mathfrak{S})$ by (A4), change variables as before, and obtain

$$I_{3\mathfrak{N}, \mathfrak{N}}(\bar{\sigma}) \sim \beta \mathfrak{S}_0 (2\pi i)^{-1} \int_{-\epsilon'}^{\epsilon'} d\zeta [1 - \mathfrak{M}_1(0) \beta i \zeta^2 \mathfrak{S}_0]^{-3\mathfrak{N}} \\ \times \exp(-23\mathfrak{N}\mathfrak{S}_0 \bar{\sigma} \beta \zeta). \quad (\text{B5})$$

Using the fact that for $T < T_c$, $h'/23\mathfrak{N} \ll 1$, this expression may be approximated as

$$I_{3\mathfrak{N}, \mathfrak{N}}(\bar{\sigma}) \sim \beta \mathfrak{S}_0 (2\pi i)^{-1} \int_{-\epsilon'}^{\epsilon'} d\zeta \exp[-\frac{1}{2} h' \mathfrak{M}_1(0) \beta \zeta^2] \\ \times \exp[-i z_2 h' \mathfrak{M}_1(0) \bar{\sigma} \zeta], \quad (\text{B6})$$

from which we obtain (4.22).